CrossMark

SOILS, SEC 5 • SOIL AND LANDSCAPE ECOLOGY • RESEARCH ARTICLE

Effects of aeolian processes on soil nutrient loss in the Gonghe Basin, Qinghai–Tibet Plateau: an experimental study

Xunming Wang[1,2] • Lili Lang[1] • Ting Hua[3] • Hui Li[3] • Caixia Zhang[3] • Wenyong Ma[1]

Abstract

Purpose The Gonghe Basin of northeastern Qinghai–Tibet Plateau is threatened by aeolian processes, soil nutrient loss, and desertification, where human activities have greatly increased over recent decades. However, the interactions between aeolian processes and soil nutrient loss remain poorly understood. Therefore, in this study, we employed a wind tunnel to simulate aeolian processes and soil nutrient loss affected by human activities such as tillage and trampling by livestock.

Materials and methods Field investigations, wind tunnel experiments, and experimental analyses were conducted to assess the impacts of human activity (wholesale destruction of vegetation) and aeolian processes on soil nutrient loss and desertification in the Gonghe Basin.

Results and discussion After grassland soil surface was disaggregated, sediments removed by high aeolian intensity (≥ 16 m s^{-1}) ranged from 294.02 to 1012.73 g m^{-2}, and wind erosion depths varied from 4.09 to 11.27 mm. High wind velocities resulted in losses of total soil organic matter (SOM) and total nitrogen (TN) by 7.56 and 0.38 kg ha^{-1}, respectively. Under very high wind velocities (≥ 22 m s^{-1}), losses of SOM and TN were 26.99 and 1.41 kg ha^{-1}, respectively. Wind tunnel experiments indicate that in the Gonghe Basin, there were no significant correlations between wind velocity and the removal of SOM and TN; however, positive correlations were observed between wind velocity and total phosphorus (TP) and total potassium (TK).

Conclusions Aeolian processes remove TK and TP from the soil surface, which has a potential impact on vegetation because that K and P are essential nutrients for plant growth. In addition, most nutrients are enriched within fine particle fraction of soil. Nutrient loss caused by aeolian processes may therefore result in the degradation of farmland and grassland, which consequently may have triggered desertification in the Gonghe Basin.

Keywords Desertification · Human activity · Qinghai–Tibet Plateau · Soil nutrient loss · Wind erosion · Wind tunnel simulation

✉ Xunming Wang
 xunming@igsnrr.ac.cn

1   Key Laboratory of Water Cycle and Related Land Surface Processes, Institute of Geographic Sciences and Natural Resources Research, Chinese Academy of Sciences, Beijing 100101, China

2   University of Chinese Academy of Sciences, Beijing 100049, China

3   Key Laboratory of Desert and Desertification, Cold and Arid Regions Environmental and Engineering Research Institute, Chinese Academy of Sciences, Lanzhou 730000, China

1 Introduction

Aeolian processes may cause the losses of nutrients and fine fractions from soil, as well as reduce water retention, which thereby may trigger desertification and reduce biomass and species richness of vegetation (e.g., the loss of herbaceous species) from the community composition (Schlesinger et al. 1990; Breshears et al. 2003; Li et al. 2006; Shao 2008; Field et al. 2012; Wang et al. 2013). The fragile ecosystems of arid and semiarid regions are highly sensitive to aeolian processes (Wang 2013), and soil nutrient loss and desertification can spread to adjacent areas, rendering them unsuitable for cultivation and animal husbandry (UNEP 1992). However, global warming has resulted in increased precipitation and temperature in some arid and semiarid areas (e.g., Ding et al. 2007;

Zhong et al. 2010), which indicates that lands unsuitable for grazing previously may now be suitable for reclamation and increased grazing intensity. Consequently, population increase and the desire to generate wealth may increase pressure for these arid and semiarid areas to be reclaimed and used for farmland and increased livestock populations. The impacts of human activity, combined with the effects of aeolian processes, have caused soil nutrient loss and desertification (Gibbens et al. 1983; Okin et al. 2006; Peters et al. 2007).

At present, most tillage practices in arid and semiarid areas of China are applied to converted grasslands, where the freshly turned soil becomes completely disaggregated in preparation for planting. In addition, the increased population density of livestock has caused damage to grassland topsoil due to the trampling by animals. The destruction of soil surface caused by agricultural conversion and trampling combined with aeolian processes results in the loss of soil particles and nutrients such as nitrogen (N), organic matter, and phosphorus (P) (Lyles 1988; Leys and McTainsh 1994; Larney et al. 1998; Yan et al. 2005; Yang et al. 2006; Alfaro 2008; Li et al. 2008, 2009).

The Qinghai–Tibet Plateau in western China covers an area of 2.57×10^6 km^2 (Zhang et al. 2002) and has a mean elevation of over 4000 m above sea level (Fig. 1). As the "Third Pole" of the globe, its ecological and environmental evolution plays an important role in regional (Li and Xue 2010) and global (Wu et al. 2007) climate change. At present, the plateau is also threatened by land degradation (e.g., Zou et al. 2002). The Gonghe Basin, located in the northeastern of the Qinghai–Tibet Plateau, is a region with high risks of soil nutrient loss and desertification (Fang et al. 1998; Feng et al. 2005). With increases in both precipitation and temperature occurring since the late 1980s, large areas of grasslands have been converted to agriculture, and grazing intensity has increased. Human activities such as tillage, trampling by farm animals, and wholesale destruction of vegetation have greatly increased over this period (Wang and Cheng 2001). However, the interactions between aeolian processes and soil nutrient loss remain poorly understood.

The occurrence of nutrient loss through aeolian processes is a key mechanism triggering desertification (Schlesinger et al. 1996; Field et al. 2012). Although nutrient loss resulting from land degradation has been documented in other regions of the world using field observations at the landscape scale (Larney et al. 1998; Hobbs and Harris 2001; Okin et al. 2009), few studies have employed field investigations combined with wind tunnel experiments to examine soil nutrient loss on the Qinghai–Tibet Plateau. Therefore, in this study, we employed a wind tunnel to simulate aeolian processes and nutrient loss on land affected by human activities such as tillage and trampling by livestock. The results can be used to appraise the significance of aeolian processes and nutrient loss and their effects on desertification in the Gonghe Basin, Qinghai–Tibet Plateau.

## 2 Materials and methods

2.1 Study site

Sampling was conducted within the Gonghe Basin at 15 sites (S01 to S15) located at 35.56–36.51° N, 99.30–101.07° E and at altitudes between 2913 and 3305 m above sea level (Fig. 1). Meteorological data from weather stations within the Gonghe Basin record a mean annual precipitation of 246 mm, annual evaporation of 1716 mm, mean wind speed of 2.7 m s^{-1}, and mean annual temperature of 2.4 °C. Vegetation cover during the growing season (i.e., May to September) varies between 5 and 20% but decreases to <5% during the windy seasons (i.e., March to June). The dominant soil at the sampling sites is meadow soil. Most areas within the basin have already been converted to farmland, and nearly all farmland surfaces are completely disaggregated by tilling during the windy season. In addition, trampling by animals has resulted in significant disturbance of grassland soil surfaces as populations of grazing livestock (e.g., sheep, goats, and yaks) have increased.

The primary grass species in the basin include *Stipa krylovii*, *Orinus thoroldii*, and *Artemisia frigida*. Secondary grass species include *Cleistogenes squarrosa*, *Ceratoides latens*, *Stipa breviflora*, *Potentilla multifida*, *Heteropappus altaicus*, *Astragalus galactites*, and *Agropyron cristatum*. Plant communities in steppe subzones are composed of *S. breviflora* and the secondary species *H. altaicus*, *Poa* sp., *Carex stenophylla*, *Sibbaldia adpressa*, *Leymus secalinus*, *Potentilla bifurca*, *Toruluria humilis*, and *Allium macrostemon*. Alpine grasslands are dominated by *Stipa purpurea*. Desert plant communities consist of *Caragana tibetica* and the secondary species *Convolvulus ammanii*, *Stellera chamaejasme*, *Dracocephalum heterophyllum*, *Achnatherum splendens*, and *Xanthopappus subacaulis*. In addition, plant communities on anchored sand dunes are characterized by *Artemisia arenaria* accompanied by *Thermopsis lanceolata*, *Corispermum hyssopifolium*, *Salsola collina*, and *Glycyrrhiza uralensis*.

2.2 Methodology

2.2.1 Field sampling and wind tunnel experiments

In August 2014, five surface soil samples were collected from each of 15 sites within the Gonghe Basin (Fig. 1). At each site separated by 100~200 m, surface samples were collected with criteria that had a smooth and intact surface (sealed, with no cracks). Soil samples were collected from the upper 20 cm since this is the maximum depth affected by human activities such as tillage and trampling by grazing livestock. One sample from each of three sites (S06, S07, and S08) was randomly selected for wind tunnel experiments, which were conducted at the Key Laboratory of Desert and Desertification of the
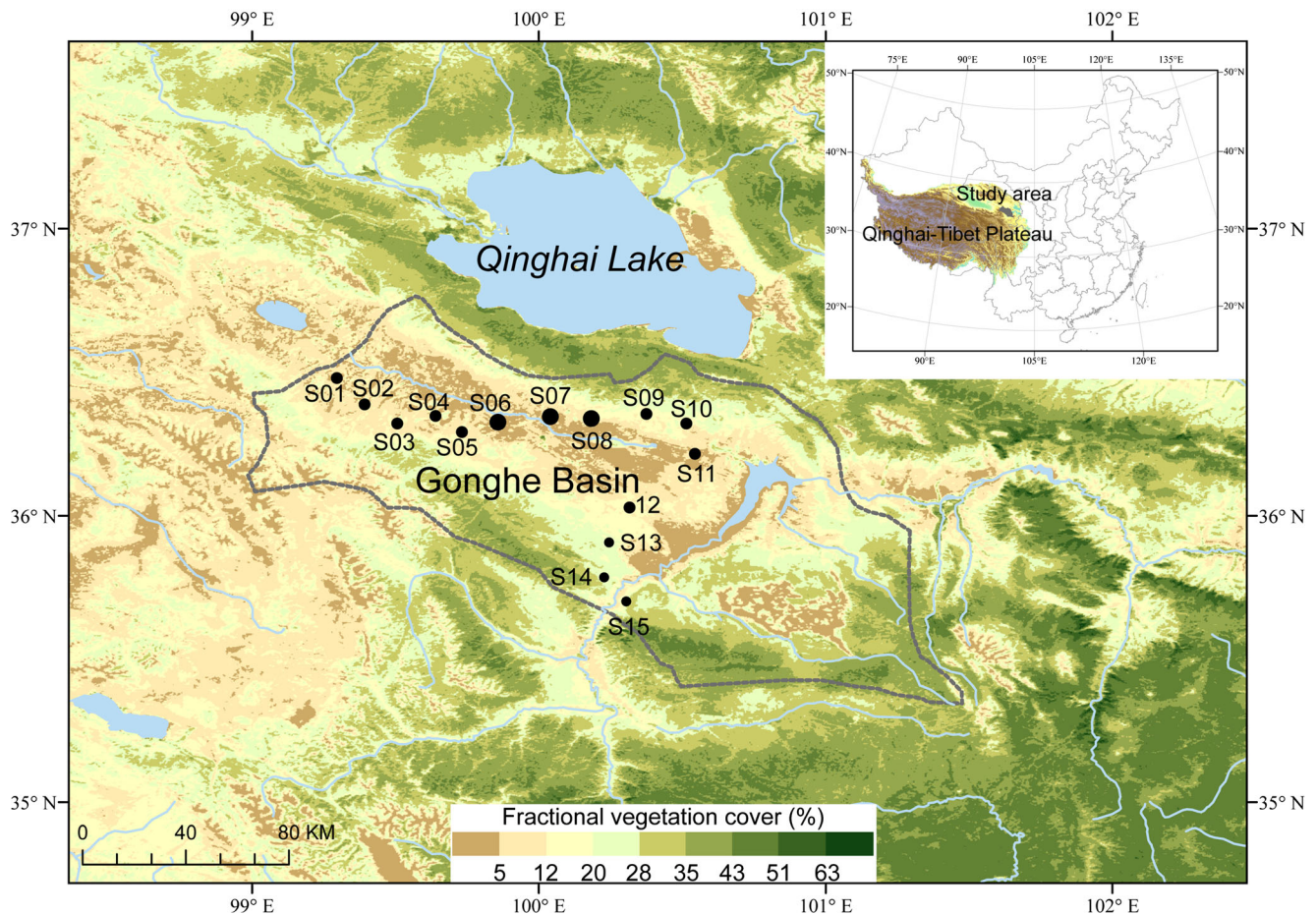
Fig. 1 Map of the Gonghe Basin. The inset shows the location of the Qinghai–Tibet Plateau within China. Sampling sites are indicated by *black circles*. Larger *black circles* indicate samples used for the wind tunnel experiments

Cold and Arid Regions Environmental and Engineering Research Institute, Chinese Academy of Sciences, Lanzhou, China. Details of the wind tunnels and related experimental processes have been described by Dong et al. (2004) and Wang et al. (2013). The soil samples were disaggregated with a hammer to simulate tillage and trampling by animals. During the wind tunnel experiments, the relative humidity was between 40 and 41%, which was similar to that in the sampling sites in August. Samples were distributed over an area of 0.3 × 1.5 m to a depth of about 2 cm thick in the wind tunnel. Windblown materials were collected by a sand trap. The trap was 30-cm wide (the same width as the surface sample) and 30-cm high and was placed 10 cm downwind of the sample. This placement allowed for collection of over 95% of the sediment transported during the wind tunnel experiment (Wang et al. 2012).

During the experiment, free-stream wind velocities of 8–22 m s^{-1} were used, increasing at intervals of 2 m s^{-1}, and the wind velocity of each run was measured using a Pitot tube (Fig. 2). Each experimental run was continued until all erodible sample particles at a given wind velocity were removed. After each run, the sand trap was emptied and the total mass of

the transported sediments was determined (balance precision, 0.001 g). All sediment transport values at a high wind speed are expressed as cumulative values that include the materials collected at all previous lower wind speeds. In addition, the wind erosion depth was measured using a three-dimensional laser scanner (EXAscan, Creaform, Canada). The scanning speed of the laser is 25,000 times per second with approximately 50,000 points per second. Resolution in the X, Y, and Z directions is 0.05 mm, and the maximum accuracy is 40 μm. After each experimental run, the three-dimensional laser scanner was used to produce a digital elevation model (DEM) of the sample surface, and the wind erosion depth was evaluated by calculating the difference between the DEMs.

2.2.2 Sample treatment and analyses

Following the wind tunnel experiments, the sediments collected in the sand trap were used for particle size analysis using a Mastersizer 2000 (Malvern, UK; sample diameter range 0.02–2000 μm) and nutrient analyses. Nutrient analyses included measurement of soil organic matter (SOM), total nitrogen (TN), total phosphorus (TP), and total potassium (TK). The
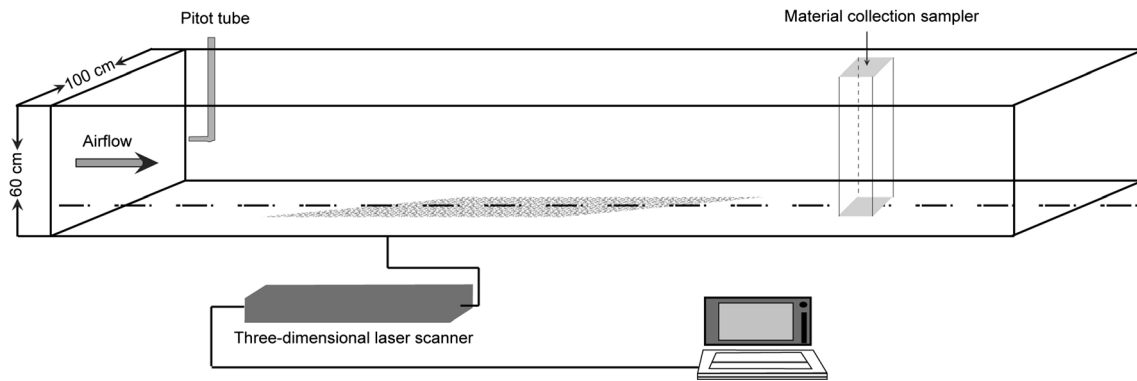
Fig. 2 Schematic diagram of the setup for the wind tunnel experiments

SOM was calculated from the soil organic carbon content, which was determined by dichromate oxidation using the Walkley Black procedure (Nelson and Sommers 1982). Total N was measured using the micro-Kjeldahl procedure, total P was measured colorimetrically using a spectrophotometer following H_2SO_4–$HClO_4$ digestion. and TK was measured using flame photometry following HF–$HClO_4$ digestion. Since higher wind velocities transport progressively larger particle sizes, all particle size fractions and nutrient contents are expressed as weighted average values for the sediments collected at a given wind velocity and all lower velocities.

3 Results

3.1 Aeolian transport intensity

A summary of wind erosion depth and intensity is showed in Table 1. The results obtained from the three-dimensional laser scanner indicate that although both erosion and deposition occurred on the sample surfaces during the wind tunnel experiments (Fig. 3), there is a close positive correlation between erosion depth and erosion intensity (Fig. 4). At low wind velocities (8–12 m s^{-1}), the mean wind erosion depth of the three samples is 0.83 mm with a mean erosion intensity of 30.6 g m^{-2}, whereas at high wind velocities (14–16 m s^{-1}), these values increase to 2.10 mm and 170.2 g m^{-2}, respectively. At very high wind velocities (18–22 m s^{-1}), the erosion depth and intensity are 5.10 mm and 420.5 g m^{-2}, respectively.

3.2 Particle sizes of the transported materials

The fine sediment fraction (<100 μm in diameter) accounted for between 50 and 90% of the original samples used in the wind tunnel experiments. At wind velocities between 8 and 22 m s^{-1}, the fine-grained fraction of the transported sediments accounted for between 30 and 90% of the total sample, and this was dependent mainly on the composition of the parent materials. Furthermore, fine fraction transport displays little variation with increasing wind velocities and in some cases even exhibits a minor increase (Fig. 5). The particle size

Table 1 Summary of data produced by wind tunnel experiments conducted on sediments collected from three sites in the Gonghe Basin

Wind velocity(m s^{-1})	S06		S07		S08	
	Wind erosion depth (mm)	Wind erosion intensity (g m^{-2})	Wind erosion depth (mm)	Wind erosion intensity (g m^{-2})	Wind erosion depth (mm)	Wind erosion intensity (g m^{-2})
8	0.56	9.36	0.72	0.00	0.55	1.13
10	0.45	47.69	0.77	2.11	1.15	17.80
12	1.39	129.87	0.21	6.13	1.72	61.16
14	2.19	251.64	0.97	18.49	1.72	119.47
16	4.26	408.04	1.21	36.07	2.25	187.58
18	6.72	601.00	1.96	62.64	3.58	247.56
20	8.21	803.84	1.04	117.56	3.97	295.71
22	11.27	1012.73	4.09	294.02	5.01	349.31

Erosion depth and intensity were measured at a range of wind velocities

Fig. 3 Spatial distribution of wind erosion depth caused by different wind velocities. Negative values of wind erosion depth indicate deposition
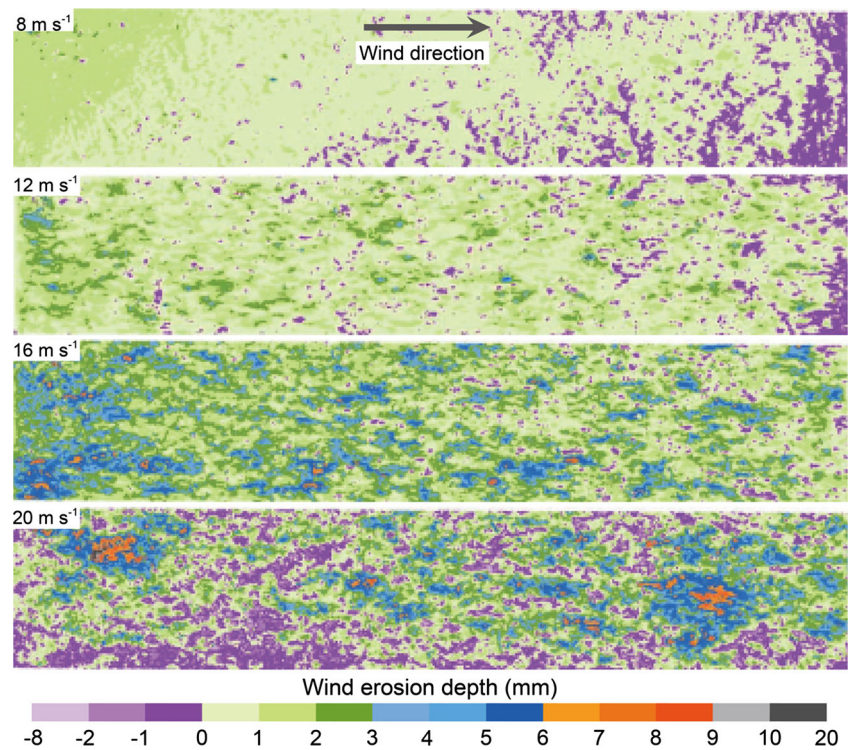

fractions of the eroded materials show that aeolian processes not only transport the fine fraction from the crushed surface soils but also transport large quantities of the coarse fraction (>100 μm in diameter), which may decrease the permeability of surface soils. In addition, after surface soils are eroded, the coarse fraction may accumulate downwind to form sand sheets or dunes, while the fine fraction may be involved in dust storms (Wang et al. 2004) that have the potential to affect

ecosystems well outside the Gonghe Basin (Reynolds et al. 2001; Soderberg and Compton 2007; Okin et al. 2008).

3.3 Nutrient loss through aeolian processes

The average SOM, TK, TP, and TN contents of the materials eroded during the wind tunnel experiments are 37.88, 14.49, 0.31, and 1.89 g kg^{-1}, respectively. The corresponding values

Fig. 4 Wind erosion intensity versus wind erosion depth. A strong linear relationship exists between the amount of material removed and the depth to which erosion takes place

$Y=0.0102X+0.5922$
$R^2=0.9683$
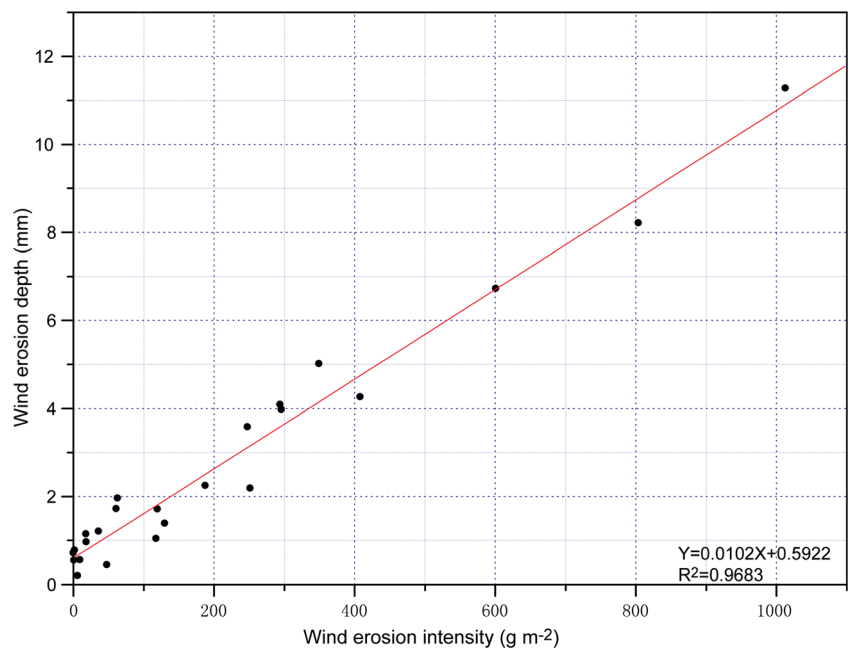
Fig. 5 Comparison of the particle size distribution of the initial surface soil samples and material transported at different wind velocities during the wind tunnel experiments
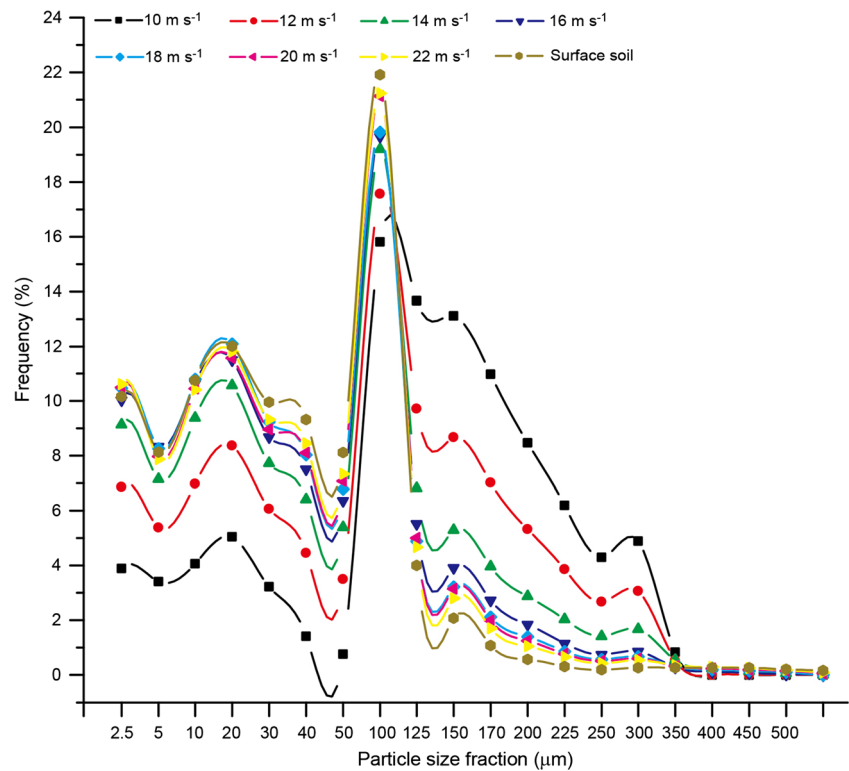
measured in the initial sediment samples are 46.95, 15.20, 0.52, and 2.65 g kg^{-1}, respectively (Table 2). These results show that compared with the initial surface soil samples, there are some slight decreases in nutrient content for the transported materials, which may be due to the fact that transported materials contain a greater proportion of low-nutrient, coarse-grained material. Statistical analysis indicates that there are significant positive correlations between wind velocity and removal of TP and TK, while no similar correlation is obtained between wind velocity and removal of SOM and TN (Fig. 6). Our results show that aeolian processes influence the correlation between nutrient contents and particle compositions. For example, there are significant correlations between particle size and the fine fraction content of SOM, TK, and TN, and the correlation coefficients are significantly higher for the transported materials (Table 3). This indicates that the fine fraction of the transported materials may have a higher nutrient content than the initial surface soils. The results of the wind tunnel experiments show that a high wind velocity (≥16 m s^{-1}) results in losses of SOM and TN totaling 7.56 and 0.38 kg ha^{-1}, respectively, and under very high wind velocities (≥22 m s^{-1}), the losses were 26.99 and 1.41 kg ha^{-1}, respectively.

4 Discussion

Given the importance of the Qinghai–Tibet Plateau for regional ecology, water supply in Asia, and the global climate

Table 2 Summary of total soil organic carbon (SOM), total phosphorous (TP), total nitrogen (TN), and total potassium (TK) contents of sedimentary material removed during the wind tunnel experiments

Sample	Wind velocity(m s^{-1})	SOM	TP	TN	TK
S06	10	6.78	12.69	0.27	0.39
	12	13.13	14.66	0.12	0.46
	14	12.60	14.25	0.20	0.26
	16	12.72	14.12	0.13	0.34
	18	12.38	14.34	0.20	0.25
	20	12.09	14.46	0.25	0.31
	22	11.82	14.55	0.27	0.39
	Surface soil	9.50	12.89	0.36	0.50
S07	16	54.42	9.62	0.19	2.88
	18	82.38	13.52	0.20	4.13
	20	98.29	15.55	0.44	4.88
	22	97.75	16.89	0.56	5.29
	Surface soil	92.10	16.83	0.66	5.16
S08	10	40.01	12.96	0.14	2.06
	12	37.86	12.86	0.34	2.17
	14	36.82	16.75	0.43	2.03
	16	40.53	16.41	0.46	2.16
	18	37.88	16.04	0.47	2.02
	20	37.18	15.68	0.42	1.98
	22	37.13	15.55	0.43	2.00
	Surface soil	39.25	15.86	0.56	2.28

Values are given as grams of nutrient per kilogram of sediment
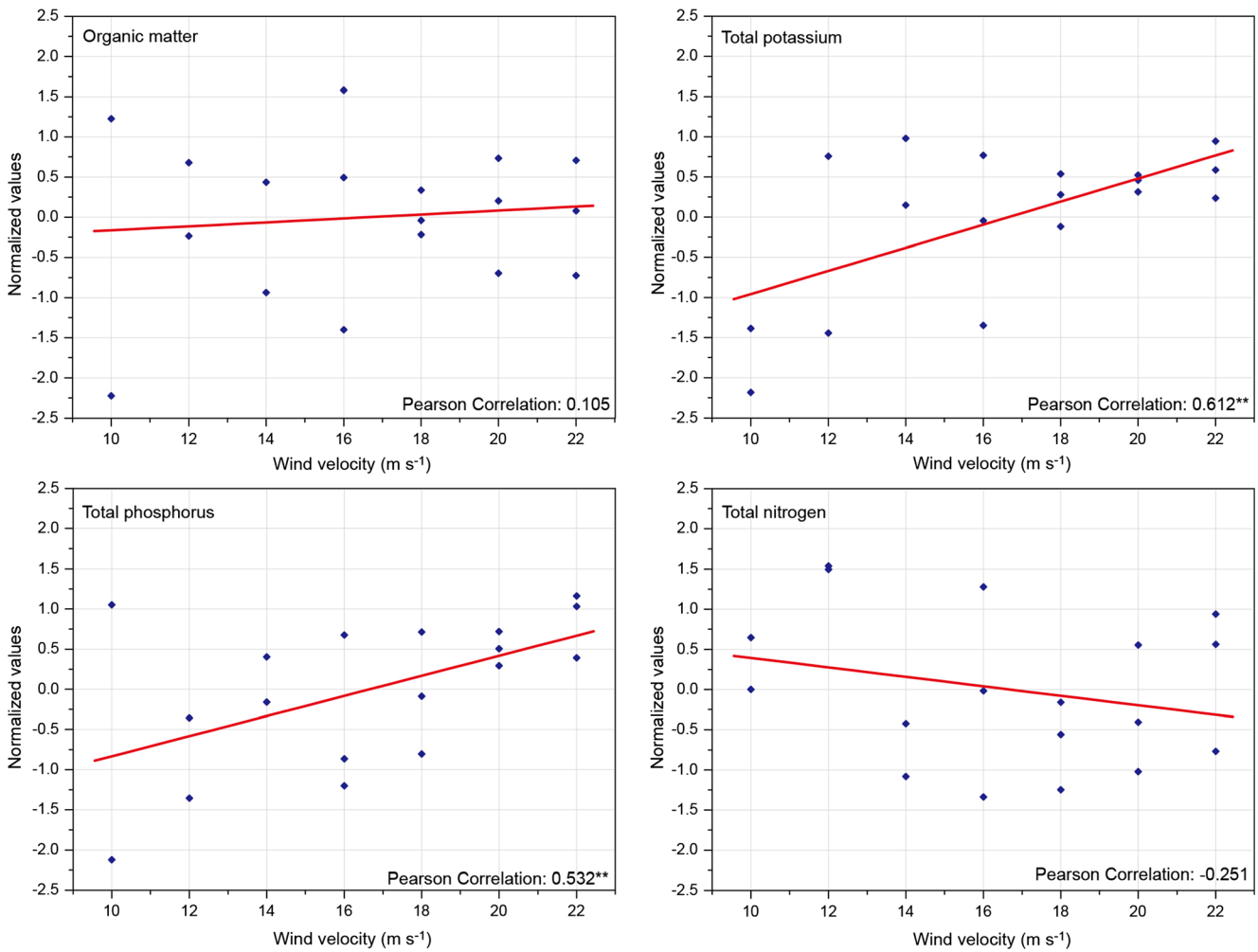
Fig. 6 Wind velocity versus normalized nutrient content. Nutrients include organic matter, total potassium, total phosphorous, and total nitrogen

system, land degradation in this region has attracted much attention. Previous studies have focused mainly on either the

effects of climate change on temporal trends in land degradation in this region (e.g., Feng et al. 2011; Wang et al. 2015) or

Table 3 Pearson's correlation coefficients between particle size fraction and soil organic matter (SOM), total nitrogen (TN), total carbon (TC), and total phosphorous (TP) of both the initial soil sample and the material transported during the wind tunnel experiments

Correlation										
		Particle fraction (µm)								
		Median	Mean	<2.5	2.5~10	10~50	50~100	100~200	200~500	500~2000
Surface soil	SOM	−0.563[a]	−0.553[a]	0.637[a]	0.532[a]	0.667[a]	0.157	−0.605[a]	−0.561[a]	−0.300[a]
	TK	−0.151	0.079	0.291[a]	0.235[a]	0.233[a]	0.064	−0.512[a]	−0.227	0.488[a]
	TP	−0.203	−0.173	0.211	0.183	0.234[a]	0.087	−0.228	−0.214	−0.053
	TN	−0.614[a]	−0.595[a]	0.691[a]	0.624[a]	0.681[a]	0.137	−0.635[a]	−0.580[a]	−0.343[a]
Transported material	SOM	−0.947[a]	−0.953[a]	0.958[a]	0.939[a]	0.955[a]	−0.486	−0.960[a]	−0.952[a]	0.789[a]
	TK	0.177	0.153	−0.133	−0.190	−0.152	0.578[a]	0.130	0.158	0.311
	TP	−0.313	−0.358	0.384	0.322	0.341	0.392	−0.381	−0.348	0.500[a]
	TN	−0.937[a]	−0.950[a]	0.957[a]	0.935[a]	0.947[a]	−0.429	−0.957[a]	−0.948[a]	0.766[a]

[a] Correlation is significant at the 0.01 level (two-tailed)

[a] Correlation is significant at the 0.05 level (two-tailed)

on the influence of one or two plant species on regional eco-logical rehabilitation (e.g., Tian et al. 2015). At present, the extent and magnitude of land degradation on the plateau re-main largely unknown, and the causes of degradation remain uncertain. The impacts of human activities such as cultivation and animal husbandry are still not sufficiently understood (e.g., Harris 2010). Some of the sites sampled in the Gonghe Basin comprised sediments containing 70.9% fine fraction (<100 μm) (Table 4). The substantial fine fraction content and vegetation cover (e.g., Livingstone and Warren 1996) ensure that high wind velocity has a low impact on intact surface soils. It is only after conversion to agriculture that the surface soils become completely disaggregated and large quantities of sediment can be eroded by wind in this region. In addition, the average contents of SOM, TK, TP, and TN in surface soil samples are 28.5, 18.7, 0.4, and 1.5 g kg^{-1}, re-spectively. The results of the wind tunnel experiments indicate that aeolian processes can trigger substantial loss of nutrients that are critical to maintaining healthy plant communities.

Over the past decades, soil nutrient loss and desertification on the Qinghai–Tibet Plateau have mainly occurred in the 1970s and mid-1980s when the intensities of human activities were low (Dong and Chen 2002; Liu et al. 2008). However, although wind velocity decreases and temperature increases over recent decades have been suitable for ecological rehabil-itation (Wang et al. 2013, 2015), increased cultivation and grazing intensity have destroyed soil structure and resulted in the export of large quantities of fine fraction and

Table 4 Summary (mean ± SD) of the particle size fractions, soil organic matter (SOM), total potassium (TK), total phosphorus (TP), and total nitrogen (TN) content of initial soil samples

Sample name		Particle size fractions (μm)								Nutrient contents (g kg^{-1})			
		Mean size	<2.5	2.5~10	10~50	50~100	100~200	200~500	500~2000	SOM	TK	TP	TN
S01	Mean	89.63	8.46	17.16	26.95	22.74	14.68	6.86	3.16	13.91	18.92	0.47	0.97
	SD	34.19	2.14	5.34	3.61	2.77	3.82	2.73	2.97	3.13	1.76	0.14	0.07
S02	Mean	264.55	2.94	4.98	12.14	15.58	19.25	27.66	17.45	13.10	23.80	0.39	0.72
	SD	44.43	1.33	1.97	4.43	1.92	1.52	5.81	4.38	5.23	1.44	0.09	0.17
S03	Mean	43.77	9.47	19.86	41.17	20.49	6.78	1.96	0.27	25.61	19.78	0.50	1.84
	SD	10.68	0.95	2.54	4.25	2.64	3.10	1.69	0.26	3.00	0.88	0.27	0.59
S04	Mean	127.16	7.86	15.07	24.10	17.33	15.87	14.76	5.02	15.91	19.87	0.38	0.99
	SD	70.40	2.69	5.28	8.75	1.93	5.53	7.14	5.13	2.35	0.79	0.20	0.17
S05	Mean	204.26	6.48	11.15	19.41	15.82	13.83	19.23	14.08	28.66	21.56	0.39	1.44
	SD	39.88	1.40	2.35	3.50	2.54	2.60	2.11	4.26	6.29	2.08	0.10	0.33
S06	**Mean**	**201.51**	**0.65**	**2.38**	**2.46**	**4.56**	**44.42**	**44.89**	**0.64**	**8.77**	**12.46**	**0.30**	**0.21**
	SD	**15.19**	**0.41**	**0.55**	**0.57**	**2.02**	**4.79**	**5.19**	**0.94**	**7.40**	**0.91**	**0.05**	**0.02**
S07	**Mean**	**119.23**	**6.77**	**13.83**	**16.94**	**14.53**	**25.66**	**21.93**	**0.33**	**28.34**	**17.34**	**0.47**	**2.08**
	SD	**34.22**	**2.44**	**5.17**	**5.80**	**2.99**	**5.93**	**9.44**	**0.26**	**9.91**	**1.82**	**0.12**	**0.92**
S08	**Mean**	**70.89**	**6.49**	**11.26**	**30.54**	**29.17**	**17.06**	**5.18**	**0.29**	**33.05**	**18.03**	**0.49**	**1.42**
	SD	**11.83**	**1.80**	**2.51**	**2.61**	**1.11**	**3.76**	**2.26**	**0.22**	**11.21**	**0.31**	**0.10**	**0.15**
S09	Mean	37.02	10.49	22.74	47.23	16.15	2.35	0.15	0.89	32.43	16.70	0.34	1.79
	SD	20.14	1.30	1.05	2.92	1.90	0.45	0.33	1.99	6.94	1.48	0.26	0.30
S10	Mean	37.27	10.88	18.37	41.97	22.36	6.10	0.32	0.00	30.68	18.25	0.27	1.65
	SD	4.62	0.66	1.12	1.90	1.62	1.74	0.70	0.01	3.51	1.77	0.26	0.11
S11	Mean	99.31	5.54	10.00	20.20	28.59	25.96	8.19	1.53	17.18	14.56	0.34	0.73
	SD	20.10	0.44	0.82	2.03	2.74	1.50	2.61	1.74	6.20	0.94	0.10	0.10
S12	Mean	120.27	6.87	12.26	30.43	16.18	11.63	19.08	3.56	26.04	19.03	0.47	1.49
	SD	10.45	0.07	0.36	1.57	1.26	0.23	1.60	1.09	3.02	3.85	0.13	0.20
S13	Mean	37.45	9.94	16.89	48.83	19.68	3.26	1.27	0.13	54.82	19.52	0.57	2.57
	SD	5.18	0.65	0.90	2.23	1.30	1.16	1.18	0.13	15.68	1.06	0.17	0.86
S14	Mean	33.96	12.46	21.46	45.46	16.35	3.31	0.52	0.44	42.50	21.00	0.63	2.35
	SD	8.08	0.55	0.53	1.66	0.70	0.55	0.52	0.96	7.99	1.84	0.07	0.16
S15	Mean	36.15	12.07	20.35	42.12	18.73	5.64	1.09	0.00	56.42	19.89	0.51	2.91
	SD	1.89	0.40	0.63	1.53	0.71	1.30	0.46	0.00	16.65	1.89	0.11	0.22

Samples utilized in this study are highlighted in bold

Fig. 7 Temporal trends in human activity around the Gonghe Basin (indicated by total cultivated area and total meat output). Data are from the Qinghai Province Statistical Yearbook
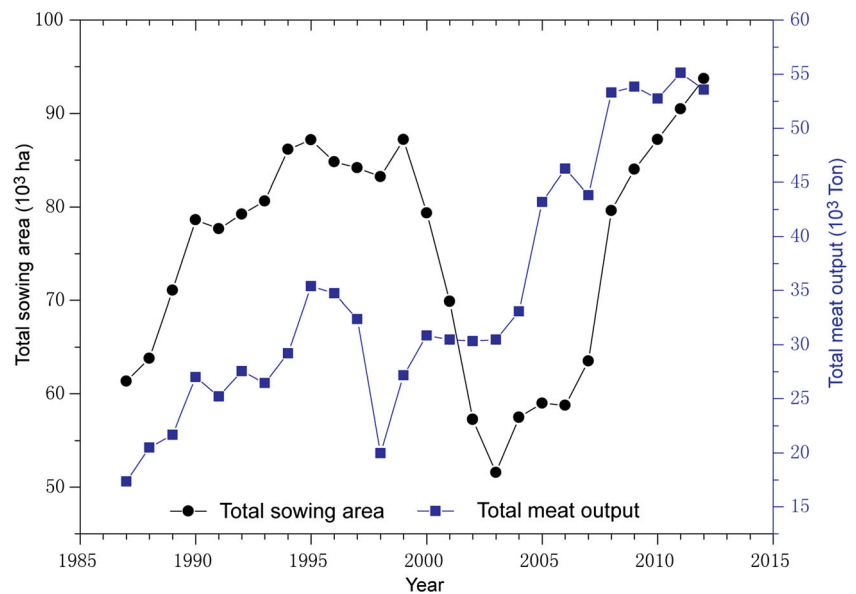
concomitant nutrient loss from the soil, which may trigger widespread desertification in the region. For example, in 1987, the total sowing area and the meat output in this region were 61,330 ha and 17,336.1 t, and in 2012, it was 93,760 ha and 53,587.0 t, respectively (Fig. 7), which showed over the past decades there was significant increase of cultivation and grazing. In this region, the increase in human activities combined with the influence of aeolian processes has led to large amounts of nutrients that are transported away from the surfaces, which consequently triggers the desertification. Therefore, although the global warming trend has fostered ecological rehabilitation on the Qinghai–Plateau from the 1990s to the present (e.g., Wang et al. 2015), significant land degradation occurrence linked to human activity after the 1990s has been observed in this region (Li et al. 2013; Yin et al. 2014).

5 Conclusions

A combination of high wind velocities and human activity (e.g., conversion to cropland and increased grazing intensity) may trigger soli nutrient loss and rapid desertification of the Gonghe Basin, Qinghai–Tibet Plateau. Our wind tunnel results demonstrate that after grassland soil surfaces are disaggregated by cultivation and animal trampling, sediment removed by low to medium wind velocities ($\leq$12 m s^{-1}) range from 6.13 to 129.87 g m^{-2} and wind erosion depth varied from 0.21 to 1.72 mm. High wind velocity ($\geq$16 m) removes between 294.02 and 1012.73 g m^{-2} of sediment, and the wind erosion depth varies between 4.09 and 11.27 mm. Furthermore, high wind velocities result in losses of total SOM and TN of 7.56 and 0.38 kg ha^{-1}, respectively, and very high wind velocities ($\geq$22 m s^{-1}) result in losses of SOM and

TN of 26.99 and 1.41 kg ha^{-1}, respectively. The data show no significant correlation between wind velocity and the proportion of SOM and TN removed; however, positive correlations are observed between wind velocity and the removal of TK and TP. These results indicate that aeolian processes may remove proportionally more TK and TP from the soil surface as wind velocity increases, which demonstrate that K and P are enriched within the fine particle fraction and that nutrient loss caused by aeolian processes may result in farmland and grassland degradation and consequently trigger desertification in the region.

References

Alfaro SC (2008) Influence of soil texture on the binding energies of fine mineral dust particles potentially released by wind erosion. Geomorphology 93:157–167

Breshears DD, Whicker JJ, Johansen MP, Pinder JE III (2003) Wind and water erosion and transport in semi-arid shrubland, grassland and forest ecosystems: quantifying dominance of horizontal wind-driven transport. Earth Surf Proc Land 28:1189–1209

Ding M, Zhang Y, Liu L, Zhang W, Wang Z, Bai W (2007) The relationship between NDVI and precipitation on the Tibetan Plateau. J Geogr Sci 17:259–268

Dong Y, Chen K (2002) Status and driving force of sandy desertification in upper reaches of Yangtze River. Resour Environ Yangtze Basin 11:84–88

Dong Z, Wang H, Liu X, Wang X (2004) The blown sand flux over a sandy surface: a wind tunnel investigation on the fetch effect. Geomorphology 57:117–127

Fang X, Li J, Zhou S, Kang S (1998) Aeolian sand deposition in the source area of Yellow River and its significance. Acta Sedimentol Sin 16:40–44

Feng J, Wang T, Qi S, Xie C (2005) Land degradation in the source region of the Yellow River, northeast Qinghai-Xizang Plateau: classification and evaluation. Environ Geol 47:459–466

Feng Y, Lu Q, Wu B, Liu H, Wang X, Che T (2011) Land-use dynamics of alpine-cold desertified area in the Qinhai-Tibetan Plateau in the last 30 years: a case study in Guinan County, Qinghai Province, China. Int J Sust Dev World Ecol 18:357–365

Field JP, Breshears DD, Whicker JJ, Zou CB (2012) Sediment capture by vegetation patches: implications for desertification and increased resource redistribution. J Geophys Res Biogeosci 117:G01033

Gibbens RP, Tromble JM, Hennessy JT, Cardenas M (1983) Soil movement in mesquite dunelands and former grasslands of southern New Mexico from 1933 to 1980. J Range Manag 36:145–148

Harris RB (2010) Rangeland degradation on the Qinghai-Tibetan plateau: a review of the evidence of its magnitude and causes. J Arid Environ 74:1–12

Hobbs RJ, Harris JA (2001) Restoration ecology: repairing the Earth's ecosystems in the new millennium. Restor Ecol 9:239–246

Larney FJ, Bullock MS, Janzen HH, Ellert BH, Olson ECS (1998) Wind erosion effects on nutrient redistribution and soil productivity. J Soil Water Conserv 53:133–140

Leys J, McTainsh G (1994) Soil loss and nutrient decline by wind erosion-cause for concern. Aust J Soil Water Conserv 7:30–40

Li JR, Okin GS, Alvarez L, Epstein H (2008) Effects of wind erosion on the spatial heterogeneity of soil nutrients in two desert grassland communities. Biogeochemistry 88:73–88

Li JR, Okin GS, Alvarez L, Epstein H (2009) Sediment deposition and soil nutrient heterogeneity in two desert grassland ecosystems, southern New Mexico. Plant Soil 319:67–84

Li Q, Xue Y (2010) Simulated impacts of land cover change on summer climate in the Tibetan Plateau. Environ Res Lett 5:015102

Li XL, Gao J, Brierley G, Qiao YM, Zhang J, Yang YW (2013) Rangeland degradation on the Qinghai-Tibet Plateau: implications for rehabilitation. Land Degrad Dev 24:72–80

Li XR, Jia XH, Dong GR (2006) Influence of desertification on vegetation pattern variations in the cold semi-arid grasslands of Qinghai-Tibet Plateau, North-west China. J Arid Environ 64:505–522

Liu J, Xu X, Shao Q (2008) Grassland degradation in the "Three-River Headwaters" region, Qinghai Province. J Geogr Sci 18:259–273

Livingstone I, Warren A (1996) Aeolian geomorphology—an introduction. Addison Wesley Longman, London

Lyles L (1988) Basic wind erosion processes. Agric Ecosyst Environ 22–23:91–101

Nelson DW, Sommers LE (1982) Total carbon, organic carbon, and organic matter. In: Page AL (ed) Methods of soil analysis. Part 2. Chemical and microbiological properties. Segoe Rd., Madison, USA, pp 539–579

Okin GS, Gillette DA, Herrick JE (2006) Multi-scale controls on and consequences of aeolian processes in landscape change in arid and semi-arid environments. J Arid Environ 65:253–275

Okin GS, Li, J, Alvarez L, Peters DPC, D'odorico P (2008) Feedbacks between aeolian processes, vegetation productivity, and nutrient flux in deserts. Joint Meeting of The Geological Society of America, Soil Science Society of America, American Society of Agronomy, Crop Science Society of America, Gulf Coast Association of Geological

Societies with the Gulf Coast Section of SEPM, Texas: George R. Brown Convention Center. pp 51–52

Okin GS, Parsons AJ, Wainwright J, Herrick JE, Bestelmeyer BT, Peters DC, Fredrickson EL (2009) Do changes in connectivity explain desertification? Bioscience 59:237–244

Peters DPC, Sala OE, Allen CD, Covich A, Brunson M (2007) Cascading events in linked ecological and socioeconomic systems. Front Ecol Environ 5:221–224

Reynolds R, Belnap J, Reheis M, Lamothe P, Luiszer F (2001) Aeolian dust in Colorado Plateau soils: nutrient inputs and recent change in source. Proceed Natl Acad Sci USA 98:7123–7127

Schlesinger WH, Raikes JA, Hartley AE, Cross AE (1996) On the spatial pattern of soil nutrients in desert ecosystems. Ecology 77:364–374

Schlesinger WH, Reynolds JF, Cunningham GL, Huenneke LF, Jarrell WM, Virginia RA, Whitford WG (1990) Biological feedbacks in global desertification. Science 247:1043–1048

Shao Y (2008) Physics and modelling of wind erosion. Springer Science & Business Media, Berlin

Soderberg K, Compton JS (2007) Dust as a nutrient source for fynbos ecosystems, South Africa. Ecosystems 10:550–561

Tian Y, Cao J, Yang X, Shan N, Shi Z (2015) Patterns of carbon allocation in a chronosequence of Caragana intermedia plantations in the Qinghai-Tibet Plateau. iForest-Biogeosci Forest 8:756–764

UNEP (United Nations Environmental Programme) (1992) World atlas of desertification. In: Middleton N, Thomas D (eds) . Edward Arnold, London

Wang G, Cheng G (2001) Characteristics of grassland and ecological changes of vegetations in the source regions of Yangtze and Yellow Rivers. J Desert Res 21:101–107

Wang X (2013) Sandy desertification: borne on the wind. Chin Sci Bull 58:2395–2403

Wang X, Dong Z, Zhang J, Liu L (2004) Modern dust storms in China: an overview. J Arid Environ 58:559–574

Wang X, Lang L, Hua T, Wang H, Zhang C, Wang Z (2012) Characteristics of the Gobi desert and their significance for dust emissions in the Ala Shan Plateau (Central Asia): an experimental study. J Arid Environ 81:35–46

Wang X, Ma W, Lang L, Hua T (2015) Controls on desertification during the early twenty-first century in the water tower region of China. Reg Environ Chang 15:735–746

Wang X, Wang G, Lang L, Hua T, Wang H (2013) Aeolian transport and sandy desertification in semiarid China: a wind tunnel approach. Land Degrad Dev 24:605–612

Wu G, Liu Y, Wang T, Wan R, Liu X, Li W, Wang Z, Zhang Q, Duan A, Liang X (2007) The influence of mechanical and thermal forcing by the Tibetan Plateau on Asian climate. J Hydrometeorol 8:770–789

Yan H, Wang S, Wang C, Zhang G, Patel N (2005) Losses of soil organic carbon under wind erosion in China. Glob Change Biol 11:828–840

Yang H, Lu Q, Wu B, Yang H, Zhang J, Lin Y (2006) Vegetation diversity and its application in sandy desert revegetation on Tibetan Plateau. J Arid Environ 65:619–631

Yin F, Deng X, Jin Q, Yuan Y, Zhao C (2014) The impacts of climate change and human activities on grassland productivity in Qinghai Province, China. Front Earth Sci 8:93–103

Zhang Y, Li B, Zheng D (2002) A discussion on the boundary and area of the Tibetan Plateau in China. Geogr Res 21:1–8

Zhong L, Ma Y, Salama MS, Su Z (2010) Assessment of vegetation dynamics and their response to variations in precipitation and temperature in the Tibetan Plateau. Clim Chang 103:519–535

Zou XY, Li S, Zhang CL, Dong GR, Dong YX, Yan P (2002) Desertification and control plan in the Tibet Autonomous Region of China. J Arid Environ 51:183–198